Mechanism of Electron Cloud Clearing with Electrodes

BNL/SNS TECHNICAL NOTE

NO. 128

L.F. Wang, D. Raparia and J. Wei

Sept. 18, 2003

COLLIDER-ACCELERATOR DEPARTMENT
BROOKHAVEN NATIONAL LABORATORY
UPTON, NEW YORK 11973

MECHANISM OF ELECTRON CLOUD CLEARING WITH ELECTRODES

L. F. Wang, D. Raparia, and J. Wei
Brookhaven national Laboratory, Upton, New York 11973-5000

ABSTRACT

Clearing electrodes have been successfully used to remove the ion from the vacuum chamber in many electron accelerators, especially in electron synchrotron light source. Electron cloud caused beam instabilities and vacuum pressure rise are becoming more and more important with the increasing beam intensity in recent years. In this paper we have explored the mechanism to clear the electron cloud by using the clearing electrode in case of the Spallation Neutron Source (SNS) accumulator ring, where strong multipacting could happen at median clearing fields.

1 INTRODUCTION

The electron-cloud instability was first reported at CERN-ISR in the coasting beam operation [1, 2] and was cured using clearing electrodes. In 1970, electron-cloud instability was observed for bunched beam in the proton synchrotron ring at Los Alamos National Laboratory (LANL-PSR) [3]. An instability, which seems to be due to the interaction of electrons and protons, has also been observed at the AGS booster [4]. Electron cloud instability has been reported in recent years in several machines, PF [5, 6], KEKB [7], PEP-II [8], BEPC[9], PS and SPS[10-11]. It was explained that beam-induced multipacting causes the electrons to accumulate inside the vacuum chamber [12, 13]. These electron clouds interact with proton or positron beam and cause beam instability. Experimental observations of electron cloud instabilities are distinctively different for “short bunches”, where multi-bunch multipacting is expected to be important (PS, SPS, and B factories) and “long bunches”, where single-bunch, trailing-edge multipacting is expected to be dominant.

In case of short bunches, the electron cloud build-up depends on the multi-bunch multipacting. Therefore, the clearing effects of electrode depend on the bunch spacing. The requirement of the clearing electrode is to clear electrons within one bunch spacing. Because there is no beam space-charge force in the bunch space, an electron can drift from one side of chamber surface to the other side during one bunch gap. A multi-wires clearing system is suggested for KEKB [14]. These systems work in both drift region and magnets. It requires a low clearing voltage and contributes to small impedance comparing with the ion clearing electrode system.

In case of long bunches, such as SNS, the electron cloud multipacting is a single bunch phenomenon. Strong multipacting happens at the tail of the bunch. Therefore, electrode must clear the electrons at the tail of the bunch by suppressing the secondary electron emission. This mechanism is different from the clearing of electron cloud in short bunch case. Although a solenoid is a good cure for electron cloud instability in the drift region, the electrode clearing system serve as a very important alternate in SNS where most of the space is occupied by magnets and other devices.

The clearing effects with electrode in SNS accumulator ring are studied using numerical method in this paper. Section 2 describes parameters and physical model of the simulation. Section 3 describes the electron multipacting with clearing electrodes. In particularly, we discuss a multipacting enhancement mechanism caused by the clearing electric field operating at an intermediate range. A conclusion is given in section 4.

2 SIMULATION PARAMETERS AND PHYSICAL MODEL

The SNS beam is assumed to be cylindrical and uniformly distribution in transverse plane. The beam and machine parameters used in simulation are shown in Table 1.

Table 1 Simulation parameters for the SNS

Parameter	Description	SNS
E (GeV)	Beam energy	1.9
C (m)	Circumference	248
N_p	Bunch population	2.05×10^{14}
a_x,a_y (mm)	Transverse beam size	28, 28
τ_b (ns)	Bunch length	700
b (cm)	Beam pipe radius	10
P_l	Proton loss rate	1.1×10^{-6}
Y	Assumed proton-electron yield	100

Protons incident on the chamber inner surfaces produce secondary electrons. Depending on the energy of the proton and the incident angle, the secondary proton-electron yield can greatly exceed unity when the incident proton is nearly parallel to the surface [15]. A proton-electron yield 100 is assumed in this study. When proton generated electrons hit the vacuum chamber, secondary electrons are emitted. The secondary electrons include three kinds of electrons, backscattered electrons, re-diffused electrons and true secondary electrons [16]. The secondary electron emission (SEY) is defined as a fraction of the number of electrons emitted from the metal surface to the total number of incident electrons. When SEY is larger than unity, number of electrons will increase exponentially. This phenomenon is called multipacting. The yield of backscattered electrons with zero incident angles is

$$\delta_e(E_0) = P_{1,e}(\infty) + [\hat{P}_{1,e} - P_{1,e}(\infty)]e^{-(\left|E_0-\hat{E}_e\right|/W)^p/p}. \quad (1)$$

Where, E_0 is the energy of the incident electron, the yield of re-diffused electrons with zero incident angles is

$$\delta_r(E_0) = P_{1,r}(\infty)[1-e^{-(E_0/E_r)^r}]. \quad (2)$$

And the yield of the true secondary electrons with zero incident angles is

$$\delta_{ts}(E_0) = \frac{s(E_0/\hat{E}_{ts})\hat{\delta}_{ts}}{s-1+(E_0/\hat{E}_{ts})^s}. \quad (3)$$

The variables in the equations (1-3) depend on the material property of the chamber surface. Figure 1 shows SEY and Table II shows the secondary emission parameters used for simulation. The true secondary parameters are based on the experimental results.

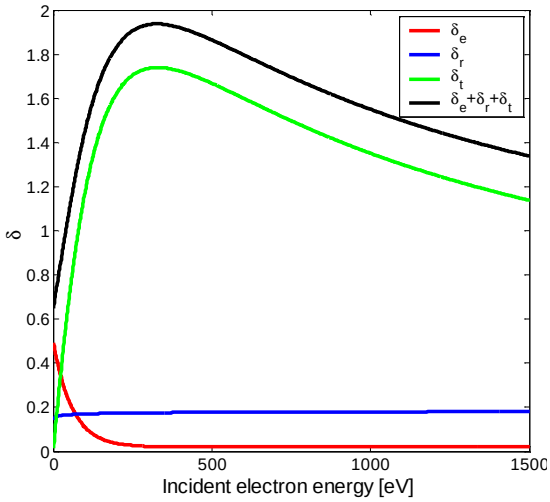

Figure 1: Secondary emission yield.

Table II: Main parameters of SEY.

Backscattered electrons	
$P_{1,e}(\infty)$	0.02
$\hat{P}_{1,e}$	0.5
$\hat{E}_e(eV)$	0
$W(eV)$	60
P	1
Re-diffused electrons	
$P_{1,r}(\infty)$	0.19
$\hat{E}_r(eV)$	0.041
R	0.104
True secondary electrons	
$\hat{E}_{ts}(eV)$	330
$\hat{\delta}_{ts}$	1.74
S	1.52553

The simulation program used in this paper is a three-dimensional particle in cell (PIC) code CLOUDLAND [17]. It includes the three-dimension electron space-charge, beam-electron interaction, various magnetic fields and electric fields. Preliminary electron is emitted when the lost proton hits the wall. The electrons move under own and beam space-charge and external fields. When an electron hits the vacuum chamber surface, it generates secondary electrons. The SEY, energy, emission angle is controlled by a statistic distribution generator obeying the experimental results. The secondary electrons may produce tertiary electrons by the same procedure. Because SEY strongly depends on the energy of the incident electrons, the multipacting is strongly depends on electron motion.

3 MULTIPACTING WITH CLEARING FIELD

In electron accelerators and storage rings, ions created by residual gas ionization, can be acutely trapped at the chamber center by the beam space-charge field. To remove these trapped ions, the necessary condition is that the electric field produced by clearing electrode should be higher than the maximum field due to beam space-charge.

Electrons are initially emitted with low energy when the lost protons hit the chamber wall surface. In principle, to suppress the electron cloud, a clearing field equal to the maximum beam space-charge field at the wall surface is required to restrain the secondary electron from emission. This requirement is more than 10,000 Volts for SNS beam. A clearing electrode with vertical uniform field is assumed in this study. The clearing field is equal to the total voltage between clearing electrodes divided by the chamber diameter.

In the case of SNS ring, where "trailing-edge multipacting" is dominant, electrons generated after the peak of the beam pulse will be accelerated towards the center of the beam and decelerated after passing through the beam center. These electrons will reach the opposite wall with an energy gain. If the energy gain is high enough, the SEY can exceed unity resulting in amplification of electron density with successive traversal across the beam pipe. Therefore, the necessary clearing field should be applied to suppress the secondary electron emission at the bunch tail. In order to find the correct clearing field, various clearing voltages were applied. The effects of the clearing electrodes were simulated using the three-dimensional particle in cell program CLOUDLAND.

Figure 2 shows the build-up of the electron cloud during the passage of one bunch with various clearing voltages. As a figure of merit, we use the peak line electron density to describe the efficiency of the clearing field. A notable feature is that the clearing efficiency is not a monotonic function of the clearing voltage as shown in Figure 3. A weak clearing field 200 Volts reduces the electron line density by a factor about 3. Subsequently, the line density increases with the increasing voltage, reaching a maximum at 2,000 Volts. The electron line density decreases again if stronger clearing fields are applied.

It is interesting that the clearing efficiency is higher for 200 Volts than for 3,000 Volts and that the multipacting is stronger with 2,000 Volts clearing field than any clearing field.

The electron motion in clearing field, as shown in Figure 4, can explain these results. The electron motion can be divided into two categories: bounce between the chamber wall surfaces with low clearing field and bounce in the neighborhood of positive clearing electrode with high clearing field.

Without any clearing field, an electron at the bunch tail bounces from one side of the wall surface to the opposite side and produces secondary electrons. The secondary electrons will bounce back again. In this case the electron energy at the wall surface ranges from 0 to 300 eV. When a low clearing voltage, for example 200 Volts, is applied, the electron still bounces between the wall surfaces. However, the clearing field can effectively reduce the electron energy at the surface closer to the negative electrode and increase it at the wall surface closer to the positive electrode. As a result, the secondary emission yield at the wall surface closer to positive electrode becomes bigger while it becomes smaller near the negative electrode due to the relationship between incident energy and SEY as shown in Figure 1. Therefore, the electron density can be reduced effectively although multipacting still happens at the surface near the positive electrode. This "alternate multipacting" mechanism ensures a low clearing field can effectively reduce the electron density.

When the clearing field increases, for example 500 Volts in Figure 4, the electron can't reach the wall surface closer to the negative electrode. Instead, it is turned back inside chamber by the clearing field and reaches to surface more close to the positive electrode than its birth location until it finally reaches

the positive electrode and moves along the vertical clearing field lines. This procedure is quite similar as the “clearing field polarization”. The destination of every electron orbit is clearing field line. The “polarization time” depends on the clearing field strength. The stronger the clearing field is, the shorter the “polarization time” is.

When an electron bounces only from one side of the chamber surface, the frequency which it hits the wall surface will reduce about half and hence electron cloud density could be smaller than without any clearing field. The effect of “half multipacting frequency” can explain the result with 500 Volts clearing voltage. Note that the electron density with 200 Volts clearing voltage is smaller than that with 500 Volts (see Figure 3). This is because the alternate multipacting results in lower density comparing with effect of “half multipacting frequency”.

With further increasing of the clearing field, for example 2,000 Volts (see Figure 4), the electron density increases because the clearing field causes the multipacting starting earlier around the beam pulse peak whereas in the low or zero field case, multipacting only could happen at the tail beam pulse. As a result, a suitable clearing field can cause stronger multipacting than without any clearing field.

The clearing field effect on the electron energy at the wall surface when it hits the wall strongly depends on the electron orbit because the electron energy receiving from the clearing field is equal to the difference of the clearing field potential between its emission and striking points. If the clearing field is weak, for example 500 Volts, the “polarization time” is long and hence the hitting location when it is forced back by the clearing field is close to its emission point. Therefore, a weak clearing field has weak effect on its energy at the wall surface during the “polarization procedure”. However, when the clearing field is stronger, the “polarization time” is shorter and electron can get more energy from the clearing field when its reach the wall surface during the “polarization procedure”. A stronger clearing field results in higher electron energy at the surface but a shorter “polarization time”, and hence, a short multipacting times. Therefore, an unsuitable clearing field, 2000 Volts (see Figure 4), can maximize the electron multipacting.

A extreme clearing field, for example 5000Volts, has weak effect on the electron energy at the wall surface except in the very short “polarization time” and it can effectively suppress the emission of secondary electrons at the bunch tail where the clearing field could be stronger than the beam space-charge field at the wall surface. Therefore, a strong clearing field can effectively reduce the electron cloud density by reducing multipacting chance at the bunch tail with weak effect at the bunch center. A clearing field equal the maximum beam space charge field at the wall surface is required for complete suppression of the multipacting.

Figure 5 and 6 shows the electron cloud transverse distribution at different time for zero and 2000 Volts clearing voltage. The distribution is azimuthally uniform in case of zero fields. However, electron cloud distributes along the clearing field line (vertical direction here) at the horizontal center due to the “polarization effect” of the clearing field.

Inside strong dipole magnets, crossed-field drifts could not eliminate the electrons, because the effects are inversely proportional to the magnetic field strength. Therefore, the clearing electric field must be applied along the magnetic field line in order to effectively repel the electron. This is also true for other strong magnetic fields. In order to excite an effective clearing field in vertical direction in a

dipole magnet, a vertical clearing field system similar as the one in the drift region can be applied. Figure 7 shows the clearing effect in dipole magnet. The clearing field always has a positive effect, which is different from the drift region case because the electron can only move along the strong magnetic field lines.

4 PRACTICAL IMPLEMENTATION

Electron generated at the stripping foil in the injection region of SNS ring is one of the main electron sources. Multi-turn charge-exchange injection is often preferred for high-intensity rings to enhance the phase-space density of the accumulated beam. Near the injection stripping-foil, a high concentration of electrons is expected with a broad energy-spectrum. With a H^- beam, the stripped electrons carry twice the current of the injecting H^- beam with a kinetic energy of $mc^2(\gamma-1)$, where γ is the relativistic factor of the H^- beam. The injecting and circulating-beams impacting on the foil produce secondary emission of electrons at low energy (tens of eV). The injecting and circulating-beam also produce knock-on electrons at a high energy (up to several MeV). Fig. 8 illustrates the collection of stripped-electrons at the SNS accumulator ring. The electrons are guided by a magnetic field and collected by a water-cooled device of heat-resistant material. The electron collector uses a carbon material attached to a water-cooled copper plate. The inner surfaces are coated with 100 nm thick TiN. A clearing electrode is installed capable of applying 10,000 Volts. The clearing field is enough for low energy electrons as studied in section 3. For high-energy electrons with energy up to several MeV, the clearing efficiency is still unknown. The combined effect of the guiding magnetic field and clearing field also need to be considered. Study of the clearing effect at injection region is under way.

At the SNS accumulator ring, the BPMs around the ring are designed to used as clearing electrodes, capable of applying a voltage of up to ±1000 Volts (see Figure 9). Such a voltage is effective with the "half multiacting frequency mechanism". However, it is not enough to completely suppress the electron cloud as explained in section 3. In order to minimize the electron cloud density, the clearing voltage should be set at the boundary of the two motion regions. It is about 200V for the parameters shown in Table 1 and 2.

5 CONCLUSION

The mechanism of clearing field applied to long bunch has been investigated for electron cloud build-up. A low clearing voltage 200 Volts or a high clearing voltage 5,000 Volts is efficient. However, the numerical study suggest that a clearing field may introduced strong multipacting at medial volatge. The strongest multipacting occurs at 2,000 Volts clearing voltage in case of SNS. The mechanism is explained by the clearing field effect on the electron energy at the wall surface. The whole clearing phenomenon can be understand from the electron motion.

6 ACKNOWLEDGMENTS

We thank Y.Y. Lee, M. Blaskiewicz, P. He, A. Fedotov, S.Y. Zhang and , R. Macek for discussions, P. Cameron, J. Brodowski, J. Tuozzolo, H. Hseuh for the discussion on practical implementation of clearing electrodes, and M. Furman for supplying data for benchmarking our code.

6 REFERENCES

1. Hereward, CERN Report No. 71-15, 1971
2. E. Keil and B. Zotter, CERN Report No. CERN-ISR-TH/71-58, 1971
3. R. J. Macek, A. Browman, D. Fitzgerald, R.C. McCrady, F. E. Merrill, M. A. Plum, T. Spickermann, T.-S. Wang, K. C. Harkay, R. Kustom, R. A. Rosenberg, J. E. Griffin, K.Y. Ng, and D.Wildman, in *Proceedings of the article Accelerator Conference, Chicago, 2001* (IEEE, Piscataway, NJ, 2001), p. 688
4. M. Blaskiewicz, in *Workshop on Instabilities of High Intensity Hadron Beams in Rings*, edited by T. Roser and S.Y. Zhang, AIP Conf. Proc. No. 496 (AIP, New York, 1999), p. 321.
5. M.Izawa, Y. Sato, and T. Toyamasu, Phys. Rev. Lett. 74, 5044-5047(1995)
6. K. Ohmi, Phys. Rev. Lett. 75, 1526-1529
7. H. Fukuma, p.1-10, CERN-2002-001(2002)
8. Sam Heifets, Proceedings of 8th advanced beam dynamics mini-workshop on two-stream instabilities in particle accelerators and storage rings, New Mexico, USA(2000)
9. Guo Z.Y., et al., 1998, Proceedings of 1st Asian particle accelerator conference. Tsukuba, Japan
10. J.M. Jimenez et al., LHC-Project-Report-632 (2003)
11. K. Cornlis, p.11-16, CERN-2002-001(2002)
12. O. Gr Ö bner, *Proceedings of the 10th International Accelerator Conference, Serpukhov, 1977* (Protvino, 1977), p. 277.
13. O. Grobner, *Proceedings of the Particle AcceleratorConference (PAC97), Vancouver, 1997* (IEEE, Piscataway, NJ, 1997), p. 3589.
14. L. Wang, H. Fukuma and S. Kurokawa, KEK-Preprint 2003-12
15. P. Thieberger, A. L. Hanson, D. B. Steski, V. Zajic, S. Y. Zhang, H. Ludewig, Phys. Rev., **A61** (1999), p. 042901.
16. M.A. Furman and M.T.F. Pivi, Physics Review Special Topics-Accelerators and Beams, Vol.5, 124404(2002).
17. L. F. Wang, H. Fukuma, K. Ohmi, S. Kurokawa and K. Oide, F. Zimmermann, Physics Review Special Topics-Accelerators and Beams, Vol. 5, 124402 (2002)
18. R. Macek, “Sources of electrons for stable beams in PSR”, PSR Technical Note, PSR-00-10; also V. Danilov et al, “Multipacting on the Trailing Edge of Proton Beam Bunches in PSR and SNS”, Workshop on Instabilities of High Intensity Hadron Beams in Rings, Upton, New York, June/July 1999, AIP Conf. Proceedings 496, p. 315.

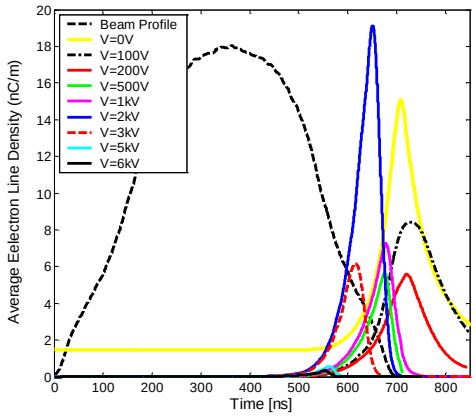

(a)

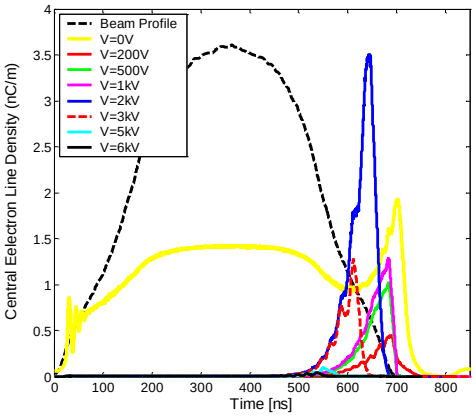

(b)

Figure 2 Electron cloud build-up with various clearing voltage in SNS drift region. (a) electron cloud line density inside vacuum chamber, (b) electron cloud line density inside beam

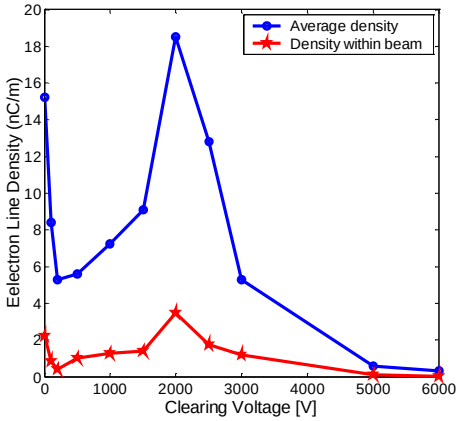

Figure 3 Peak electron cloud line density with various clearing potential in SNS drift region

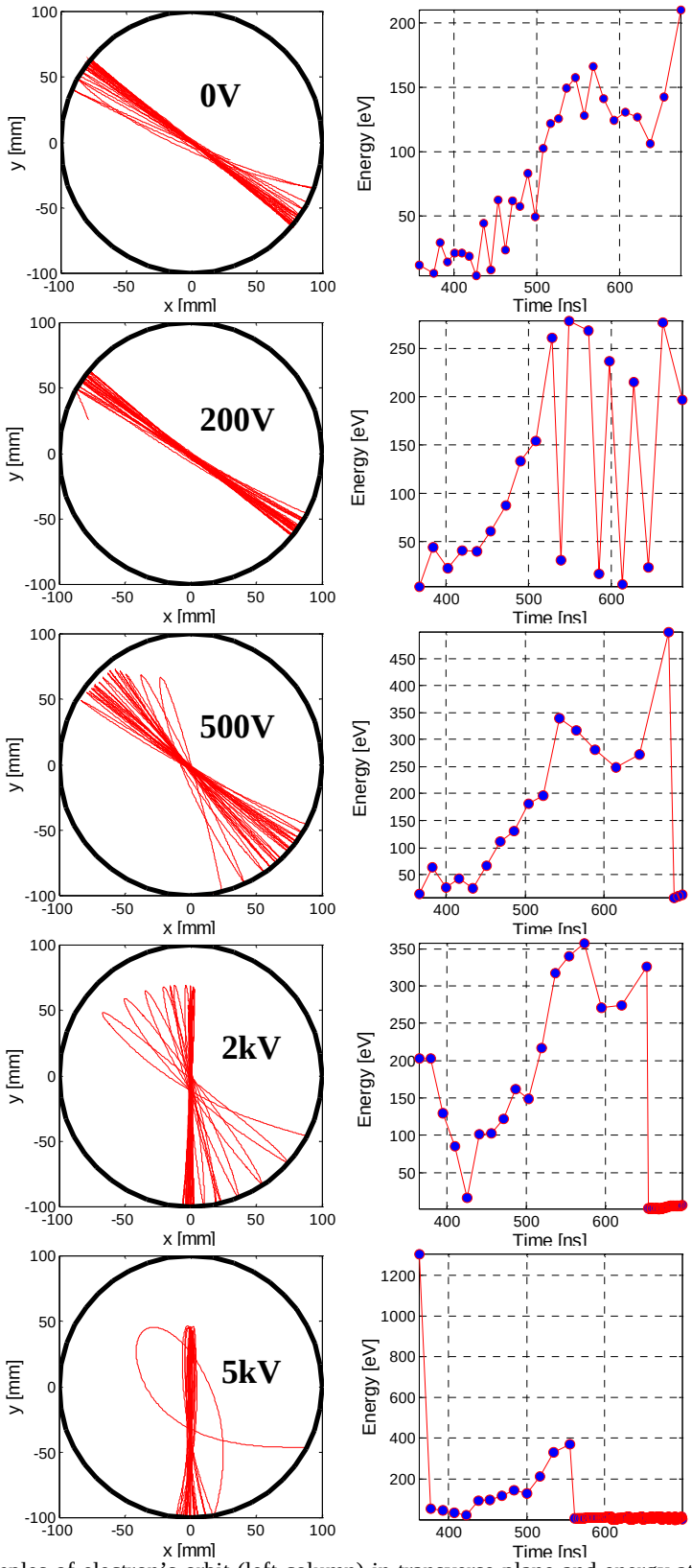

Figure 4 Examples of electron's orbit (left column) in transverse plane and energy at the wall surface (right column) with various clearing voltages. The red lines in the left column is orbit, solid black lines shows the vacuum chamber shape.

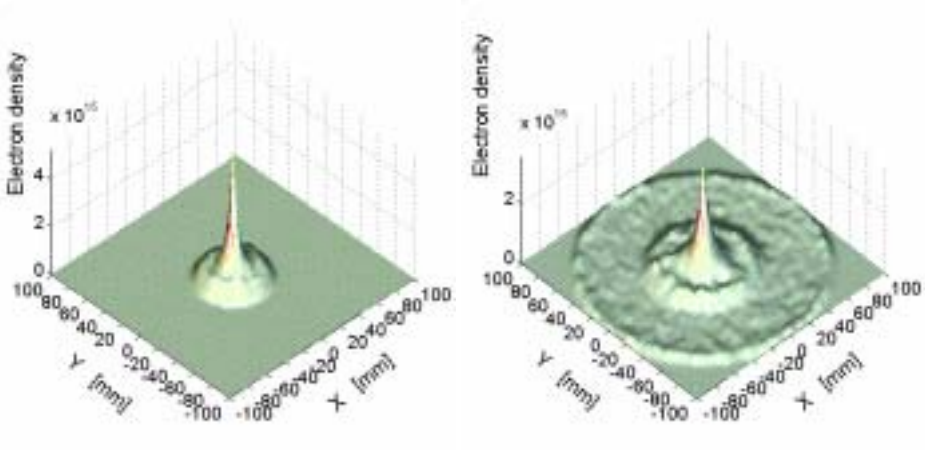

(a) (b)

Figure 5: Electron distribution at 350 ns (a) and 630 ns (b) with zero clearing potential.

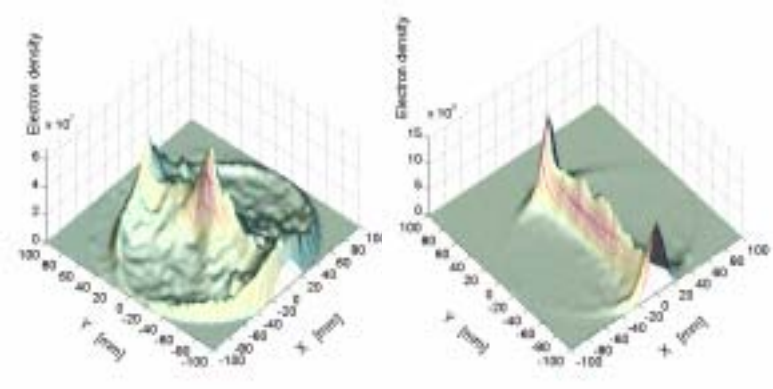

(a) (b)

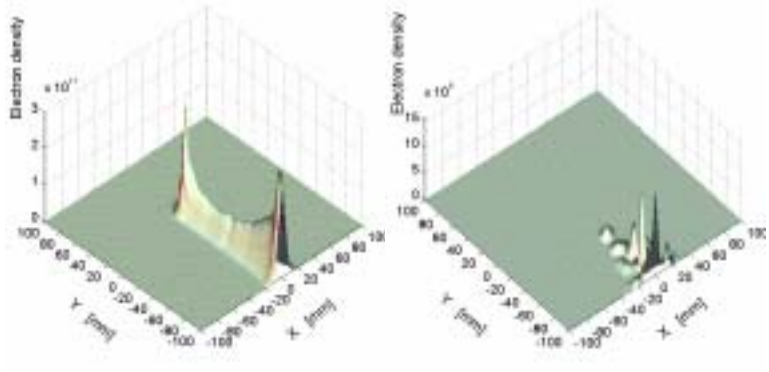

(c) (d)

Figure 6: Electron distribution with 2000Volts clearing potentials at different time.

(a) 350 ns, (b) 560 ns, (c) 630 ns and (d) 700 ns.

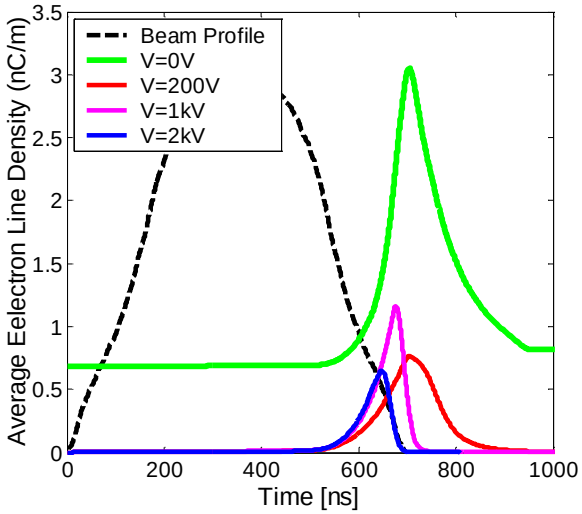

Figure 7: Electron cloud build-up with various clearing voltage in SNS dipole magnet

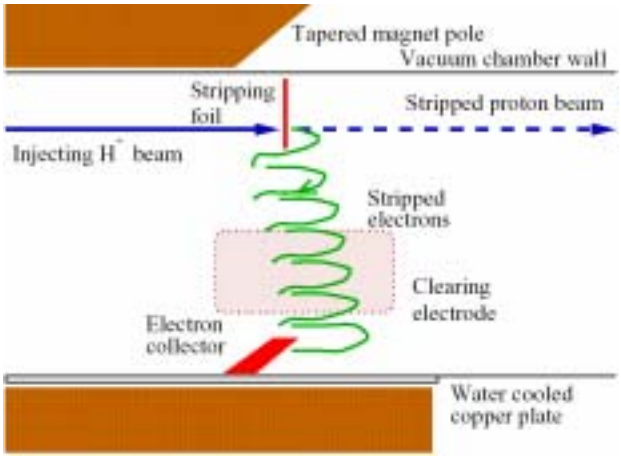

Figure 8: Collection of stripped electrons during the injection of H^- beam at the SNS ring.

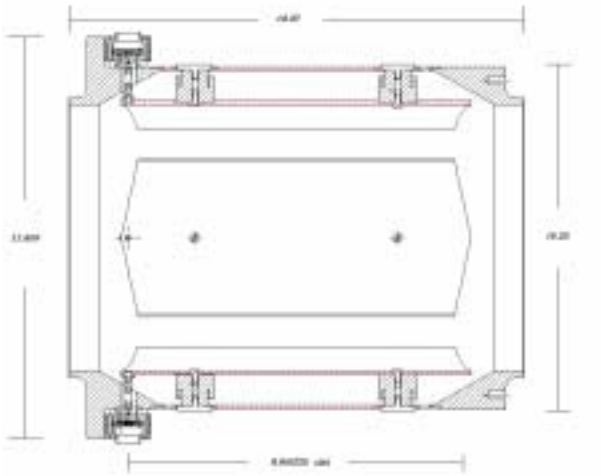

Figure 9: Schematics of the floating-ground BPM designed for the SNS accumulator ring. A voltage of about 1000 Volts can be applied for the clearing of the electron cloud.